Novel insights in thrombosis pathophysiology using Mice with Impaired anticoagulation

Heestermans, M.

3

Role of Platelets, Neutrophils, and Factor XII in Spontaneous Venous Thrombosis in Mice

Marco Heestermans
Salam Salloum-Asfar
Daniela Salvatori
El Houari Laghmani
Brenda M Luken
Sacha S Zeerleder
Henri MH Spronk
Suzanne Korporaal
Gerry TM Wagenaar
Pieter H Reitsma
Bart JM van Vlijmen

Manuscript under revision

ABSTRACT

Recently, platelets, neutrophils, and factor XII have been implicated as important players in the pathophysiology of venous thrombosis. Their role became evident in mouse models where surgical handlings were used to provoke thrombosis. Inhibition of anticoagulation in mice using small interfering (si) RNA targeting *Serpinc1* and *Proc* also results in a thrombotic phenotype, which is spontaneous (no additional triggers), and reproducibly results in clots in the large veins of the head and fibrin deposition in the liver. This thrombotic phenotype is fatal, but can be fully rescued by thrombin inhibition. In the present study, this model was used to investigate the role of platelets, neutrophils, and factor XII. After administration of siRNAs targeting *Serpinc1* and *Proc*, antibody-mediated depletion of platelets fully abrogated the clinical features as well as microscopic aspects in the head. This was corroborated by strongly reduced fibrin deposition in the liver. Whereas neutrophils were abundant in siRNA-triggered thrombotic lesions, antibody-mediated depletion of circulating Ly6G-positive neutrophils did not affect onset, severity, or thrombus morphology. In addition, absence of circulating neutrophils did not affect quantitative liver fibrin deposition. Remarkably, siRNA-mediated depletion of plasma factor XII accelerated the onset of the clinical phenotype; mice were more severely affected, with more severe thrombotic lesions. In conclusion, in the present study, onset and severity of the thrombotic phenotype are dependent on the presence of platelets, but not circulating neutrophils. Unexpectedly, factor XII has a protective effect. This study challenges the proposed roles of neutrophils and factor XII in venous thrombosis pathophysiology.

INTRODUCTION

Venous thrombosis (VT) is a complex disease and its pathogenesis is incompletely understood. Recently, it is recognized that cellular components of the blood may contribute to the initiation and propagation of VT (1, 2). Mouse models have been important tools to study the pathogenesis of VT. In models based on flow restriction (stasis), induced by partial ligation of the inferior vena cava, and in the absence of any vascular and/or endothelial damage, it was shown by von Brühl and others that blood leukocytes were actively recruited to the inflamed venous vessel wall, resulting in initiation and propagation of VT (1-3). An interplay between these recruited blood cells (mainly platelets and neutrophils) and coagulation factor XII (FXII) appeared critical for thrombus formation (1).

Although this mouse model for VT proved valuable for identifying potential novel players in VT, the role of blood stasis, hypoxia, and endothelial activation may be overestimated compared to the human situation of VT (1, 3). Particularly in cases where imbalanced coagulation, either as a result of environmental conditions or genetic background, is the driving risk factor for VT (4, 5). It cannot be excluded that in the model used by von Brühl et al. the numerous surgical handlings required to establish stasis in the inferior vena cava contribute to a proinflammatory state. Furthermore, the retrograde formation of thrombi is an important difference between that model and the human situation.

Recently, we described a mouse model with an acute imbalance in coagulation, achieved by strong inhibition of the hepatic expression of antithrombin (*Serpinc1*) and Protein C (*Proc*) using synthetic small interfering (si) RNA (6). Inhibition of these anticoagulants resulted in a highly reproducible, siRNA dose-dependent, and thrombin-dependent thrombotic coagulopathy, which, without interventions, is fatal. Likely due to vascular bed-specific hemostasis and local flow characteristics (7), (fibrin-layered) thrombi were reproducibly formed in large veins in the head (in the masseter and mandibular area). Moreover, fibrin was deposited in the liver and plasma fibrinogen was consumed resulting in prolonged clotting times. As thrombus initiation and propagation in this model required no additional triggers other than inhibition of anticoagulant gene expression (achieved by intravenous siRNA injection), we used this model to further evaluate the role of platelets, neutrophils, and FXII in the initiation and propagation of VT.

METHODS

Animal experiments

C57BL/6J female mice (18-20 g) were purchased from Charles River (Maastricht, the Netherlands). siRNAs targeting mouse antithrombin (si*Serpinc1, cat*. #S62673, Ambion, Life Technologies, Carlsbad (CA), USA), protein C (si*Proc*, cat. #S72192) and a control siNEG (cat. #4404020) were designed and/or used as described previously (6). For siRNA-mediated silencing of coagulation factor XII *(F12)*, RNA-strand sequences were; sense: 5'-CCACAAAUGCAUCCACAAAtt-3' and antisense: 5'-UUUGUGGAUGCAUUUGUGGtg-3' (cat. #S81735). For *in vivo* use, siRNAs were complexed with Invivofectamine® 2.0 (Invitrogen, Life Technologies) and injected intravenously (tail vein) at a dose of 5.75 mg/siRNA/kg body weight. This dose reproducibly results in spontaneous macrovascular VT limited to the head (in the masseter and mandibular area), irrespective of sex and strain. siRNA-complexes targeting *F12* were injected 24 hours before si*Serpinc1*/si*Proc* treatment.

For platelet depletion a rat monoclonal antibody against mouse GP1b (#R300, Emfret, Würzburg, Germany) was used. Depletion of neutrophils was achieved using a rat monoclonal antibody targeting mouse Ly6G (clone 1A8, Biolegend, San Diego, USA), and a rat isotype control IgG (clone RTK2758, Biolegend) as a control. Antibodies were injected intravenously (5 mg/kg body weight) 6 hours after si*Serpinc1*/si*Proc* injection, unless indicated differently.

Animals were sacrificed, and citrated blood and liver were collected as described (8, 9). Mouse heads were fixated in 4% formaldehyde. All experimental procedures were approved by the institutional animal welfare committee.

Liver and blood analyses

Liver transcript levels of *Serpinc1*, *Proc*, and *F12* were determined using qPCR, with *Actb* as a house-keeping gene (8, 9). siRNA-mediated hepatic silencing of *Serpinc1* and *Proc* silencing was routinely confirmed[6]. Liver fibrin deposition was determined by immunoblotting using the monoclonal antibody 59D8 (10).

Blood neutrophil numbers were measured using flow cytometry (LSR II, BD Biosciences, San José, USA) using αLy6G-phycoerythrobilin (clone 1A8, BD Biosciences). Platelet and neutrophil numbers were determined with a hematology analyzer (Sysmex XE-2100). *Ex vivo* platelet activity (with and without stimulus) was determined as described (11). Plasma FXII activity was determined using an activated partial thromboplastin time-based assay using FXII-deficient human plasma, using C57BL/6J mouse pool plasma for calibration (9). Plasma nucleosome levels and thrombin generation (tissue factor and ellagic acid-induced) were determined as described (12, 13).

Phenotype assessment

The spontaneous thrombotic phenotype following si*Serpinc1*/si*Proc* injection has been described extensively before (6), and developed in all mice 2 to 3 days after siRNA injection. Because of the severe nature of the clinical symptoms that accompanied the thrombotic phenotype, animals were sacrificed 72 hours after si*Serpinc1*/si*Proc* injection, unless indicated differently.

After sacrifice (not including animal perfusion), formalin-fixed heads were decalcified (in 20% formic acid), dehydrated, paraffin-embedded, and sectioned. After analysis of coronal serial sections of the head and neck, sections (4 µm) were made starting directly caudal of the eyes, since this area was most clearly and reproducibly affected and thrombi in large veins were found here (in si*Serpinc1*/si*Proc* injected animals). Selected sections were stained using hematoxylin and eosin or according to Carstairs' methodology (14). Severity of the phenotype at the microscopic level was scored based on the presence and extent of thrombotic lesions, subcutaneous and intramuscular bleeding, and subcutaneous edema in the entire section (figure S4). Incidence and appearance of thrombotic lesions in the selected sections was categorized and scored (see figure S6 for elaborate explanation).

Immunohistochemistry

Paraffin embedded coronal sections of the head area (i.e. serial sections of those described above) were stained with a rat monoclonal anti-mouse Ly6G (clone A8, Biolegend). For detection, a horseradish peroxidase (HRP) labelled rabbit anti-rat IgG antibody was used (Dako, Agilent Technologies, Glostrup, Denmark). HRP activity was detected using diaminobenzidine (Dako).

RESULTS

Platelets are crucial for spontaneous thrombosis

In si*Serpinc1*/si*Proc*-treated animals, in thrombi of the mandibular area of the head, platelets (Carstairs' light blue positive) appeared abundantly present in thrombi and also co-localized both with leukocytes (dark blue/purple) and fibrin (bright red/pink, see figure S1A). Additionally, a reduction in blood platelet counts coincided with increased liver fibrin deposition and development of the clinical features of the thrombotic coagulopathy (figures S1B). Flow cytometry analysis showed that the circulating platelets did not display a significant increase of surface activation markers before onset of the thrombotic phenotype (figure S1C). To investigate the role of platelets during spontaneous thrombotic coagulopathy following silencing of anticoagulant genes *Serpinc1* and *Proc*, platelets were depleted using an antibody targeting mouse GP1b, 6 hours after si*Serpinc1*/si*Proc* injection. Successful platelet depletion (no platelets detectable in whole blood) was confirmed in a dedicated pilot study (data not shown) and in a parallel group

that did not receive si*Serpinc1*/si*Proc* (figure 1A; median: 616x10^9 platelets/L (range: 554, 642 minimum and maximum, respectively) vs. 0x10^9 platelets/L (0, 7), *P*=0.036).

Fully in line with previous observations (6), animals treated with siRNAs targeting *Serpinc1* and *Proc* and subsequently injected with saline (designated as -αGP1b in figure 1) developed the typical clinical features of the thrombotic coagulopathy within three days: Mice developed unilateral lesions around the eye and swellings in the head. Moreover, they became lethargic, unresponsive to stimuli, hypothermic, and showed a significant loss in body weight. One of the affected mice died before it could be included for further analysis. In contrast, si*Serpinc1*/si*Proc* +αGP1b mice (+αGP1b in figure 1) appeared fully healthy (figure 1B), and did not experience weight loss compared to the si*Serpinc1*/si*Proc* -αGP1b group, which emphasizes their retained health (figure S2A; -2.05g (-3.05, 0.15) vs. 0.13g (-0.99, 0.77), *P*=0.043). Strikingly, platelet depletion at a later time point (si*Serpinc1*/si*Proc*-treated mice received αGP1b when the first two mice presented the clinical features of the thrombotic phenotype) also fully rescued mice from thrombotic coagulopathy. All mice in the reference group became affected as expected (9/9 vs. 2/9, -αGP1b and +αGP1b, respectively. *P*=0.002).

On a microscopic level, in the si*Serpinc1*/si*Proc* -αGP1b group, thrombi were found in all mice in the larger and smaller veins of the selected coronal sections of the head (figure 1C and S3). Moreover, extensive multifocal red blood cells extravasations (hemorrhages) were present especially in the masseter and mandibular area, with associated subcutaneous edema (7 of 7 mice). In contrast, in the si*Serpinc1*/si*Proc* +αGP1b mice, neither thrombi nor notable injuries were observed (figure 1D, S3, and S5A). When the presence of thrombi was scored, two types of thrombi were defined based on their composition and structure (figure 1E and figure S6). Interestingly, one mouse that was not clinically affected (yet) did appear to have thrombi in a vessel in the investigated coronal section of the head (figure 1B, -αGP1b). In contrast, no mice in the si*Serpinc1*/si*Proc* +αGP1b group appeared to have any thrombi. In line with these observations, liver fibrin deposition was strongly and significantly reduced in the si*Serpinc1*/si*Proc* +αGP1b group (figure 1F; 75.7 ng/mg (21.40, 143.9) vs. 9.46 ng/mg (6.34, 21.69), *P*=0.001), although liver fibrin levels were above background level observed in control animals solely injected with control siRNA (siNEG, figure 1F; 4.50 ng/mg (3.13, 5.72), *P*<0.001).

Circulating neutrophils are not a major mediator of spontaneous thrombosis

Mice were depleted of neutrophils 6 hours after si*Serpinc1*/si*Proc* injection, using an antibody targeting the neutrophil-specific Ly6G membrane protein (+αLy6G in figure 2). In this experimental setup, an isotype IgG antibody was used in the group not depleted of neutrophils (-αLy6G in figure 2). Flow cytometry analysis confirmed in a dedicated experiment that the Ly6G-positive i.e. neutrophil population was fully absent in the circulation up to 4 days after antibody

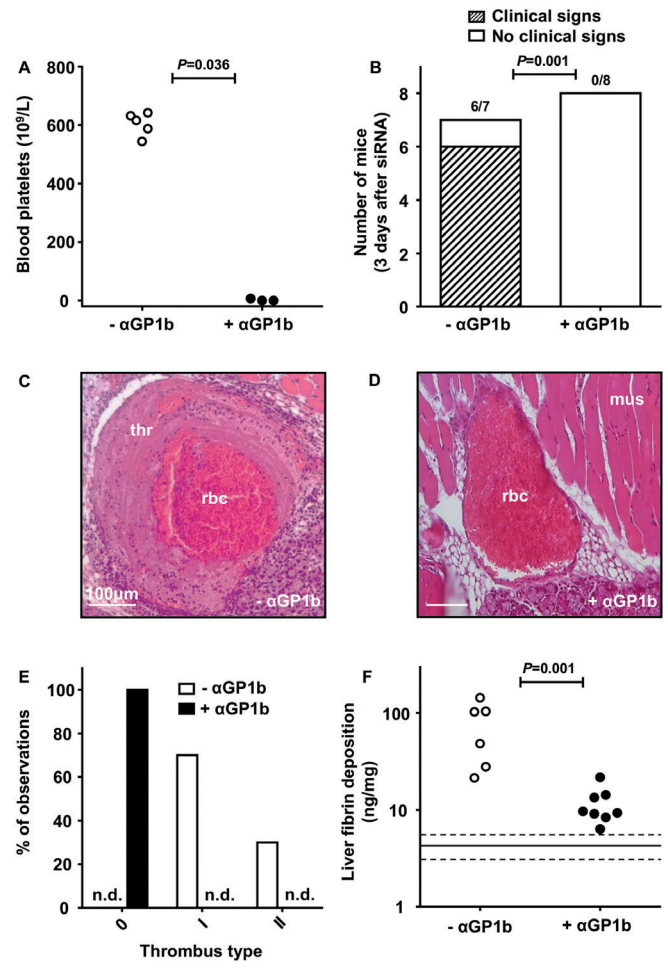

Figure 1 | Depletion of platelets prevents thrombotic coagulopathy following siRNA-mediated hepatic knockdown of *Serpinc1* and *Proc*. A, Blood platelets numbers in mice from a parallel group not receiving siRNA 3 days after injection with saline (open circles) or with a rat monoclonal antibody targeting mouse GP1b (black circles). *P*=0.036, Mann Whitney Rank-sum test. B, Scoring of the clinical phenotype in mice treated with siRNAs targeting *Serpinc1* and *Proc*. Animals showing characteristic clinical coagulopathy (hatched bar) and animals unaffected (open bars) 3 days after siRNA treatment (end of experiment). One of the mice from the -αGP1b-group died because of the thrombotic coagulopathy. *P*=0.001, Fisher-exact test. C/D, Representative thrombus identified in a vein in the control group (-αGP1b, panel C), and a representative vein in the platelet depleted group (+αGP1b, panel D) in H&E stained sections. thr: Thrombus with typical fibrin layers, rbc: postmortem clotted blood rich in red blood cells, mus: Striated muscle tissue. White bars indicate 100µm. E, Scoring for the presence of thrombi. 0: no thrombi found, I + II: thrombi categories based on structure and layering (see method section and figure S4). Open bars: -αGP1b (n=10), black bar: +αGP1b (n=16), n.d. not detected. F, Levels of fibrin deposition in the liver of the platelet depleted group (+αGP1b) and the control group (-αGP1b). *P*=0.001, Mann Whitney Rank-sum test. Solid and dashed lines indicate fibrin levels found in solely siNEG injected C57BL/6J female mice (median and range, resp. 4.50 ng/mg (3.13, 5.72)). Data are presented as the median with the range (minimum and maximum, respectively).

injection (data not shown). Using the same approach, we again did not detect neutrophils in the circulation in the si*Serpinc1*/si*Proc* +αLy6G group one day after antibody injection and one day before onset of the phenotype (figure S7). Additionally, after sacrifice the absence of neutrophils in the si*Serpinc1*/si*Proc* +αLy6G treated group was confirmed (figure 2A; 720 neutrophils/μL (320, 1120) vs. 0 neutrophils/μL (0, 280), *P*<0.001).

si*Serpinc1*/si*Proc* treated mice in both the neutrophil-depleted (si*Serpinc1*/si*Proc* +αLy6G) and in the isotype IgG treated group (si*Serpinc1*/si*Proc* -αLy6G) developed the typical clinical signs of the thrombotic coagulopathy (figure 2B). Moreover, body weight was lowered for mice in both groups to a comparable extent (figure S2B; -0.85g (-3.24, 0.13) vs. -2.48g (-3.61, -0.31), *P*=0.132). On a microscopic level, coronal sections of the head were analyzed and in both groups thrombi were found in large veins, as well as hemorrhages and edema. Severity scoring yielded no differences in severity (figure S5B). In the si*Serpinc1*/si*Proc* -αLy6G group, Ly6G-positive cells were abundantly present in thrombi and followed the alignment of structures identified as fibrin and adhered to the thrombotic venous vessel wall (figure 2C). Ly6G-positive cells in thrombi were absent in the si*Serpinc1*/si*Proc* +αLy6G group (although in some animals strongly reduced Ly6G-positive signal was found in some cells in the thrombus, see figure 2D). Generally, thrombus leukocyte density was affected after neutrophil depletion (compare in figures 2C, 2D, and S8). Depletion of neutrophils did not significantly affect the organizational structure and lining of the thrombi (figure 2E and S6). In line, increased liver fibrin deposition compared to an siNEG control group of mice was evident, but no differences between both si*Serpinc1*/si*Proc* treated groups were observed (figure 2F; 67.87 ng/mg (9.28, 587.5) vs. 51.92 ng/mg (10.94, 3126), *P*=0.931).

To investigate whether the thrombotic coagulopathy following si*Serpinc1*/si*Proc* injection coincided with the formation of neutrophil extracellular traps (NETs), and whether neutrophil depletion affects NET formation, we determined plasma levels of extracellular nucleosomes as a NET biomarker (12). Plasma nucleosome levels were moderately but significantly increased (*P*=0.003 and *P*<0.001, respectively si*Serpinc1*/si*Proc* -αLy6G and si*Serpinc1*/si*Proc* +αLy6G) in mice with the thrombotic coagulopathy when compared to untreated mice (figure S9). However, no differences were found in plasma from mice with or without detectable neutrophils in the circulation (si*Serpinc1*/si*Proc* -αLy6G: 46 U/mL (7, 756), si*Serpinc1*/si*Proc* +αLy6G: 59 U/mL (10, 771), *P*=0.448), suggesting extracellular nucleosomes detected in plasma of thrombotic animals were not derived from neutrophils.

Reduced FXII propagates development of the spontaneous venous thrombosis

The role of FXII was studied using an siRNA approach (si*F12*). For mice treated with si*F12* only (without si*Serpinc1*/si*Proc* injections), FXII plasma activity was decreased (72 after siRNA injection) by 87.3% (93.2-81.4, *P*=0.029) as compared to pool plasma, while FXII levels of the siNEG treated

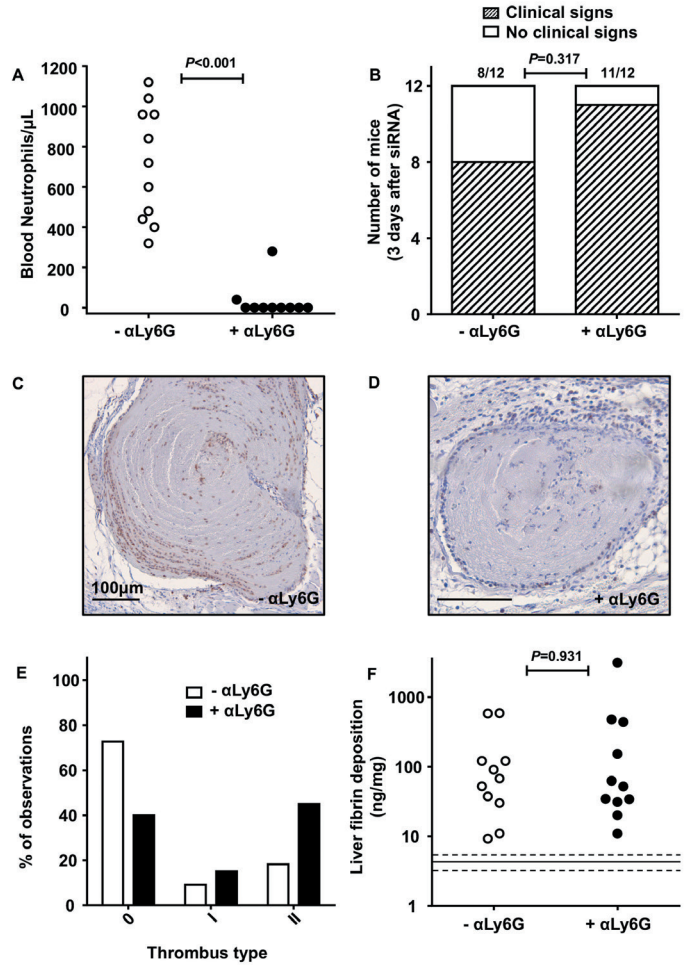

Figure 2 | Depletion of neutrophils does not influence progression of thrombotic coagulopathy following siRNA-mediated hepatic knockdown of *Serpinc1* and *Proc*. A, Blood neutrophils numbers in mice 3 days after injection with a rat monoclonal antibody targeting mouse Ly6G (black circles) or a rat IgG control (open circles). *P*<0.001, Mann Whitney Rank-sum test. B, Scoring of the clinical phenotype in mice treated with siRNAs targeting *Serpinc1* and *Proc*. Animals showing characteristic clinical signs (hatched bar) and animals unaffected (open bars) 3 days after siRNA treatment (end of experiment). One of the mice in both groups (-αLy6G and +αLy6G) died because of the thrombotic coagulopathy. *P*=0.317, Fisher-exact test. C/D, Ly6G staining of thrombi found in sections of the head, in the -αLy6G (panel C) and +αLy6G (panel D). Hematoxylin was used for counterstaining, black lines indicate 100 μm. E, Scoring for the presence of thrombi. 0: no thrombi found, I + II: thrombi categories based on structure and layering. Open bars: -αLy6G (n=22), black bars: +αLy6G (n=20). F, Levels of fibrin deposition in the liver of the neutrophil depleted group (+αLy6G) and the control group (-αLy6G). *P*=0.931, Mann Whitney Rank-sum test. Solid and dashed lines indicate fibrin levels found in solely siNEG injected C57BL/6J female mice (median and range, resp. 4.50 ng/mg (3.13, 5.72)). Data are presented as the median with the range (minimum and maximum, respectively).

group were in the normal range (figure 3A; 110.9% (101.0, 118.9) of pool plasma). Moreover, groups treated with si*Serpinc1*/si*Proc* in combination with si*F12* or siNEG (designated +si*F12* and -si*F12* in figure 3, respectively) were analyzed for hepatic *F12* transcript levels (after sacrifice). A reduction in hepatic *F12* transcript of 86.0% (87.9-84.9, *P*<0.001) was observed in the si*Serpinc1*/si*Proc* +si*F12* group.

To investigate whether thrombin generation (TG) was altered in mice with lower levels of FXII, we performed a TG assay on plasma from mice 48 hours after si*F12* treatment i.e. 24 hours after si*Serpinc1*/si*Proc* injection, with ellagic acid (contact-activation initiated) or tissue factor as triggers for TG. At this time point, animals did not show any clinical singularities and were completely healthy. Endogenous thrombin potential values did not differ between si*Serpinc1*/si*Proc* -si*F12* and si*Serpinc1*/si*Proc* +si*F12* groups in both measurements (ellagic acid: 1019 nM.min (518, 1810) vs. 1488 nM.min (552, 1689), -si*F12* and +si*F12*, resp. *P*=0.151; tissue factor: 919 nM.min (670, 2073) vs. 807 nM.min (613, 949), -si*F12* and +si*F12*, resp. *P*=0.193), and no other differences were observed in TG curves (data not shown). In line, low FXII did not significantly affect APTT (as determined in siNEG and siF12-only animals; 38.7s (32.5-38.9) vs. 39.4s (38.3-45.9), *P*=0.40, 1:1 diluted plasma).

Remarkably, with lower plasma levels of FXII, mice treated with siRNAs against *Serpinc1* and *Proc* (si*Serpinc1*/si*Proc* +si*F12*) developed earlier and more severely clinical symptoms of thrombosis compared to the siNEG treated group (si*Serpinc1*/si*Proc* -si*F12*, figure 3B, 4/10 vs. 9/9, *P*=0.011). Because the onset of the clinical symptoms was premature (within 48 hours after si*Serpinc1*/si*Proc* treatment) compared to previous experiments, we stopped the experiment and sacrificed animals 2 days after si*Serpinc1*/si*Proc* treatment. To emphasize the difference between both groups, FXII-lowered mice experienced significantly more body weight loss during the experiment (figure S2C; -0.05 g (-1.60, 0.60) vs. -2.30 g (-3.10, -1.60), *P*<0.001). This surprising outcome was confirmed in a second independent experiment with an identical setup, where again in large majority of mice in the si*Serpinc1*/si*Proc* +si*F12* group onset of the typical coagulopathy was evident 2 days after si*Serpinc1*/si*Proc* injection, while animals in the si*Serpinc1*/si*Proc* -si*F12* group were healthy at this early time point (0/8 and 7/8, *P*=0.001, body weight gain: -0.35 g (-0.70, 0.50) vs. -0.95 g (-1.90, -0.20), *P*=0.004).

On a microscopic level, thrombus formation, hemorrhages, and edema were more severe in the si*Serpinc1*/si*Proc* +si*F12* group compared to the si*Serpinc1*/si*Proc* -si*F12* group (figure 3C and 3D as an example, figure S5C for severity scoring). Blinded analysis of the coronal sections yielded thrombotic lesions characterized by structured fibrin layering were present in the si*Serpinc1*/si*Proc* -si*F12* group, but absent in the si*Serpinc1*/si*Proc* +si*F12* group (figure 3E). Instead, in the si*Serpinc1*/si*Proc* +si*F12* group lesions were observed mostly in disrupted veins consisting of

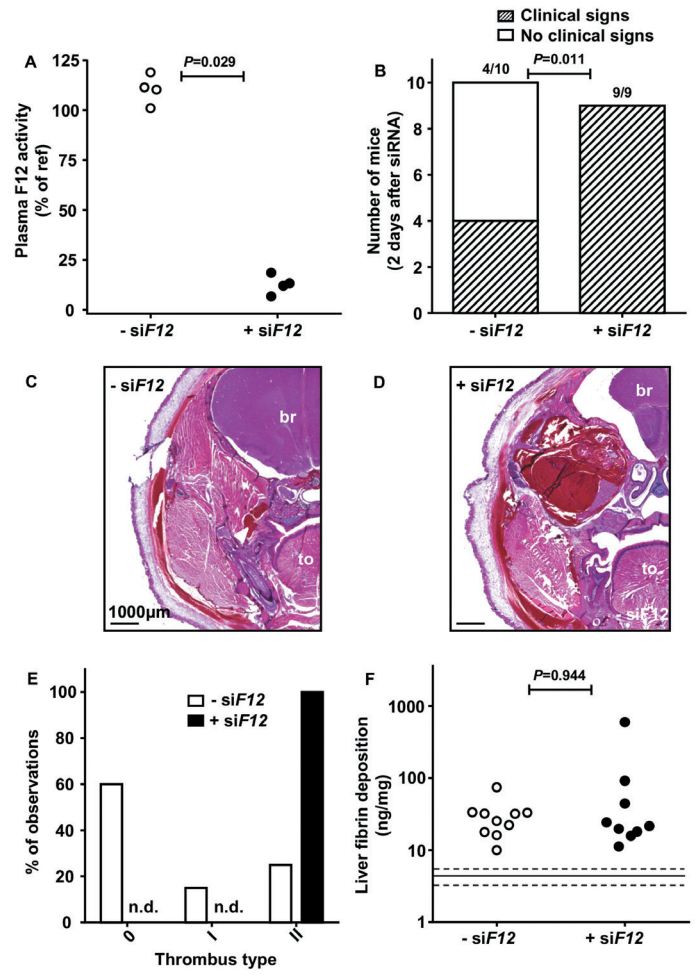

Figure 3 | siRNA-mediated hepatic knockdown of *F12* worsens thrombotic coagulopathy induced by knockdown of *Serpinc1* and *Proc*. A, Plasma FXII activity in mice 3 days after injection with an siRNA targeting *F12* (black circles) or siNEG (open circles). *P*=0.029, Mann Whitney Rank-sum test. Normal pool plasma was used as an internal reference. B, Clinical phenotype in mice treated with siRNAs targeting *Serpinc1* and *Proc*. Animals showing characteristic clinical signs (hatched bar) and animals unaffected (open bars) 2 days after siRNA treatment (end of experiment). *P*=0.011, Fisher-exact test. C/D, Representative H&E stained coronal head sections from the –si*F12* group (panel C) and the +si*F12* group (panel D). For orientation of the selected section, br: Brain, to: Tongue, arrowheads indicate extravasated red blood cells. Black lines indicate 1000µm. E, Scoring for the presence of thrombi. 0: no thrombi found, I + II: thrombi categories based on structure and layering. Open bars: -si*F12* (n=20), black bars: +si*F12* (n=18), n.d. not detected. F, Levels of fibrin deposition in the liver of the FXII deficient group (+si*F12*) and the control group (-si*F12*). *P*=0.944, Mann Whitney Rank-sum test. Solid and dashed lines indicate fibrin levels found in solely siNEG injected C57BL/6J female mice (median and range, resp. 7.13 ng/mg (6.10, 7.96)). Data are presented as the median with the range (minimum and maximum, respectively).

mixtures of red blood cells and structures identified as eosin-positive fibrin, lacking a typical layered structure (type II thrombotic lesions). However, detailed histological analysis of the thrombi did not yield clues that low FXII levels uniquely impacts clot structure. Despite the more severe clinical phenotype and more severe lesions observed microscopically in the si*Serpinc1*/si*Proc* +si*F12* group, liver fibrin deposition levels were comparable for si*Serpinc1*/si*Proc* treated groups (figure 3F; 28.71 ng/mg (9.95, 74.57) and 21.55 ng/mg (11.24, 596.1), –si*F12* and +si*F12*, respectively, *P*=0.944).

DISCUSSION

In the present study, we investigated the role of platelets, neutrophils, and factor XII in the pathophysiology of VT using a mouse model that features spontaneous onset of VT i.e. in a thrombosis model that does not require additional triggers or handlings other than silencing expression of two liver-derived anticoagulants through simple intravenous injection of synthetic siRNAs. In this model, platelets, but not neutrophils, were found to be rate-limiting in thrombus formation, while low plasma FXII was found to aggravate spontaneous thrombosis. The results of this study therefore challenge the proposed roles of neutrophils and FXII in VT pathophysiology.

Platelets, recently identified as major players in experimental VT in a ligation model, are recruited early after flow restriction and are involved in stabilization and accumulation of innate immune cells (1). Thrombus formation does not take place in the absence of platelets. Also in the present study, rescue from thrombotic coagulopathy after platelet depletion was complete. These observations provide further evidence for an important role of platelets during experimental VT, and is in line with previous studies (1, 15).

In the present model, the thrombotic coagulopathy rapidly progresses with a transition within hours from a condition where animals have no thrombotic lesions detectable in the head and minimal liver fibrin deposition, towards a condition where veins in the head are occluded with thrombi and liver fibrin deposition is evident. We now suggest that platelets are particularly important for the burst of fibrin and thrombus formation, but not for initial fibrin formation. This is supported by 1) thrombi were not detected in platelet-depleted mice, while liver fibrin deposition was found to be increased compared to baseline level (figure 1F). Also 2) late platelet depletion just before the expected onset of the thrombotic phenotype fully rescues. Finally 3), von Willebrand factor (VWF), a protein important for platelet adherence but not for massive fibrin formation, is not involved in si*Serpinc1*/si*Proc* induced thrombosis. VWF-deficient animals did not respond differently upon silencing of anticoagulation as compared to animals that express VWF (4 out of 6 *Vwf-/-* mice vs 5 out of 6 *Vwf+/+* control mice macroscopically and microscopically

affected within 72 hours after si*Serpinc1*/si*Proc* injection). Overall, the present study confirms an important but different role for platelets as posed previous in VT pathophysiology, and thereby further evidence to investigate antiplatelet therapy as prophylactic treatment against (recurrent) VT (16, 17).

Neutrophils have been linked in recent years to play a role in VT, via a specialized cell death program where NETs are released (18, 19). During thrombus formation in a mouse model of experimental VT, NETs released upon neutrophil recruitment to the (proinflammatory) vessel wall are indispensable (1). The role of neutrophils became evident using an antibody-mediated depletion strategy identical to the method used in this study (depletion of Ly6G-positive cells). Also for the electrolytic inferior vena cava model of VT, where the vena cava is directly activated by an electric current causing endothelial damage, it was demonstrated vein wall neutrophils were the most common cell type present in acute VT (20). Moreover, neutrophils and NETs have also been identified in human specimens of VT (21, 22).

When VT follows silencing of anticoagulant genes, Ly6G-positive neutrophils were abundantly present within the thrombi, seemingly recruited and aligned to the fibrin layers, which is consistent with previous observations (1, 2). However, in our model, neutrophils were not rate-limiting in thrombus formation. We were unable to detect any phenotypically relevant impact of neutrophil depletion, which is in strong contrast with previous observations. Hence, the proposed role of neutrophils in the thrombosis pathophysiology does not hold true for conditions where endothelial activation and/or vessel wall inflammation are considered absent (i.e. not triggered by surgical handlings). Therefore, we expect a less vital role for neutrophils in humans when manifestation of VT is clearly associated with thrombophilia.

The abundance and specific alignment of neutrophils in the spontaneously formed thrombi in the head (figure 2C) suggest that neutrophils are not innocent bystanders during thrombosis. Neutrophils may have an active role in the inflammatory process associated with thrombosis, possibly once the thrombus is formed. The finding of occasional Ly6G+ cells in thrombi in the si*Serpinc1*/si*Proc* +αLy6G group (while undetectable in the circulation) suggests that the formed thrombi are strong triggers for neutrophil recruitment, possibly from sources other than the circulation. Overall, our data indicate that the role of neutrophils in thrombosis may depend on the trigger, and encourage studies on the role of neutrophils after thrombus formation.

FXII has been a therapeutic candidate for treatment of VT since it may be involved in thrombus formation, but not essentially in haemostasis (2, 23, 24). In our model of spontaneous VT, strong reduction in plasma FXII was achieved through silencing the hepatic transcript, resulting in reduced plasma protein activity 10-20% of control. At these levels, plasma performs normally in

thrombin generation assays following intrinsic and extrinsic stimulation and produces normal aPTTs. Surprisingly, we observed an effect of low plasma FXII on thrombus formation: We observed a faster onset and more severe thrombotic coagulopathy in mice with low levels of FXII.

We are puzzled by this observation, and considered three potential mechanisms for FXII. First, we considered low FXII-enhanced secondary bleeding tendency as a mechanism underlying the observed more severe coagulopathy. In the experiment that reproduced the exacerbating effect of low FXII in spontaneous thrombosis, microscopic analysis of coronal sections of the head area showed that animals of the *siSerpinc1/siProc* -si*F12* group did not all develop the thrombotic phenotype (yet) after 2 days, while all si*Serpinc1*/si*Proc* +si*F12* animals did. In other words, lowering FXII levels seemed to accelerate thrombosis onset, which argues against an effect of low FXII through enhancing the secondary bleedings in the head.

Secondly, we considered changes in the fibrinolytic pathway as a mechanism by which low FXII modulates spontaneous VT. FXII also contributes to clot structure and fibrinolysis (25-30). FXII can interact with pro-fibrinolytic factors (25) and deficiency of FXII causes less dense/stiff clots (26, 27). In line, activation of FXII with polyphosphates in normal whole blood, but not FXII-deficient plasma, increased clot firmness (28, 29). Detailed histological analysis of the thrombi formed during our experiments however did not yield clues whether low FXII indeed uniquely impacts clot structure. Of note, the present thrombosis model was not particularly sensitive to alterations in fibrinolysis, as the antifibrinolytic agent tranexamic acid did not affect the onset or progression of si*Serpinc1*/si*Proc*-mediated thrombosis (at a dose 2.5g tranexamic acid/kg/day starting before siRNA injections, data not shown). This argues against an impact of low FXII levels on thrombosis onset and severity through altered clot formation and/or fibrinolysis.

Thirdly, we considered changes in the kinin/kallikrein pathway as a mechanism by which low FXII may modulates spontaneous VT (31). We investigated the impact of low FXII on edema formation. Edema in the masseter and mandibular area is a clear macroscopically visible feature of spontaneous thrombosis. We hypothesized that low FXII reduces kallikrein formation and consequently the release of bradykinin, which hinders formation of edema (opposite to hereditary angioedema type III, where a gain of function in FXII induces edema formation[32]. In thrombotic mice with low FXII impaired edema formation would worsen the phenotypic response, through an inability to deal with intravenous pressure following thrombotic occlusion. Quantitation of edema in the head (measured by the thickness of the edemic dermis in coronal sections of the head) did not yield clues that low FXII altered edema formation (data not shown). As antibodies and/or chromogenic substrates for detection of (activity) mouse components of the kallikrein/kinin pathway are lacking, we are not able to provide additional data further exploring kinin/kallikrein pathway as a mechanism of low FXII in spontaneous thrombosis.

We conclude that in the present VT model based on lowering anticoagulation factors, FXII inhibition does not rescue the thrombotic phenotype. Further studies are needed to clarify the mechanisms of thrombus formation and the role of FXII and related proteins (like coagulation factor XI) in thrombosis following impaired anticoagulation.

In this report we challenge the proposed essential roles for platelets, neutrophils, and FXII in VT pathogenesis. Mouse models where thrombosis is induced by stenosis-induced stasis, leading to hypoxia and endothelial activation, demonstrate a crucial role for these factors, but our data imply neutrophils and FXII are not essential in thrombus formation when impaired anticoagulation is the driving force. Hence, targeting neutrophils or FXII for therapeutic purposes is an interesting thought, but might not be applicable for treatment of every case of VT. On the other hand, our study provides further rationale for antiplatelet therapy as prophylactic treatment for (recurrent) VT.

REFERENCES

1. von Bruhl ML, Stark K, Steinhart A et al. Monocytes, neutrophils, and platelets cooperate to initiate and propagate venous thrombosis in mice in vivo. *Journal of Experimental Medicine* 2012;209:819-835.
2. Geddings JE, Mackman N. New players in haemostasis and thrombosis. *Thrombosis and Haemostasis* 2014;111:570-574.
3. Geddings J, Aleman MM, Wolberg A et al. Strengths and weaknesses of a new mouse model of thrombosis induced by inferior vena cava stenosis: communication from the SSC of the ISTH. *Journal of Thrombosis and Haemostasis* 2014;12:571-573.
4. Martinelli I. Risk factors in venous thromboembolism. *Thrombosis and Haemostasis* 2001;86:395-403.
5. Dahlback B. Advances in understanding pathogenic mechanisms of thrombophilic disorders. *Blood* 2008;112:19-27.
6. Safdar H, Cheung KL, Salvatori D et al. Acute and severe coagulopathy in adult mice following silencing of hepatic antithrombin and protein C production. *Blood* 2013;121:4413-4416.
7. Rosenberg RD, Aird WC. Vascular-bed - Specific hemostasis and hypercoagulable states. *New England Journal of Medicine* 1999;340:1555-1564.
8. Safdar H, Cheung KL, Vos HL et al. Modulation of Mouse Coagulation Gene Transcription following Acute In Vivo Delivery of Synthetic Small Interfering RNAs Targeting HNF4 alpha and C/EBP alpha. *Plos One* 2012;7:
9. Cleuren ACA, Van der Linden IK, De Visser YP et al. 17 alpha-Ethinylestradiol rapidly alters transcript levels of murine coagulation genes via estrogen receptor alpha. *Journal of Thrombosis and Haemostasis* 2010;8:1838-1846.
10. De Visser YP, Walther FJ, Laghmani EH, van der Laarse A, Wagenaar GT. Apelin Attenuates Pulmonary Inflammation and Fibrin Deposition in Neonatal Hyperoxic Lung Injury. *American Journal of Respiratory and Critical Care Medicine* 2009;179:
11. Kooijman S, Meurs I, van der Stoep M et al. Hematopoietic alpha 7 nicotinic acetylcholine receptor deficiency increases inflammation and platelet activation status, but does not aggravate atherosclerosis. *Journal of Thrombosis and Haemostasis* 2015;13:126-135.
12. Zeerleder S, Zwart B, Velthuis HT et al. A plasma nucleosome releasing factor (NRF) with serine protease activity is instrumental in removal of nucleosomes from secondary necrotic cells. *Febs Letters* 2007;581:5382-5388.
13. Hemker HC, Giesen P, AlDieri R et al. The Calibrated Automated Thrombogram (CAT): A universal routine test for hyper- and hypocoagulability. *Pathophysiology of Haemostasis and Thrombosis* 2002;32: 249-253.
14. Mangin P, Yap CL, Nonne C et al. Thrombin overcomes the thrombosis defect associated with platelet GPVI/FcR gamma deficiency. *Blood* 2006;107:4346-4353.
15. Brill A, Fuchs TA, Chauhan AK et al. von Willebrand factor-mediated platelet adhesion is critical for deep vein thrombosis in mouse models. *Blood* 2011;117:1400-1407.
16. Becattini C, Agnelli G, Schenone A et al. Aspirin for Preventing the Recurrence of Venous Thromboembolism. *New England Journal of Medicine* 2012;366:1959-1967.
17. Warkentin TE. Aspirin for Dual Prevention of Venous and Arterial Thrombosis. *New England Journal of Medicine* 2012;367:2039-2041.
18. Brinkmann V, Zychlinsky A. Neutrophil extracellular traps: Is immunity the second function of chromatin? *Journal of Cell Biology* 2012;198:773-783.
19. Martinod K, Wagner DD. Thrombosis: tangled up in NETs. *Blood* 2014;123:2768-2776.
20. Diaz JA, Alvarado CM, Wrobleski SK et al. The electrolytic inferior vena cava model (EIM) to study thrombogenesis and thrombus resolution with continuous blood flow in the mouse. *Thrombosis and Haemostasis* 2013;109:1158-1169.
21. Savchenko AS, Martinod K, Seidman MA et al. Neutrophil extracellular traps form predominantly during the organizing stage of human venous thromboembolism development. *Journal of Thrombosis and Haemostasis* 2014;12:860-870.
22. van Montfoort ML, Stephan F, Lauw MN et al. Circulating Nucleosomes and Neutrophil Activation As Risk Factors for Deep Vein Thrombosis. *Blood* 2012;120:
23. Gailani D, Renne T. Intrinsic pathway of coagulation and arterial thrombosis. *Arteriosclerosis Thrombosis and Vascular Biology* 2007;27:2507-2513.
24. Muller F, Gailani D, Renne T. Factor XI and XII as antithrombotic targets. *Current Opinion in Hematology* 2011;18:349-355.
25. Konings J, Hoving LR, Ariens RS et al. The role of activated coagulation factor XII in overall clot stability and fibrinolysis. *Thromb.Res.* 2015;136:474-480.
26. Konings J, Govers-Riemslag JWP, Philippou H et al. Factor XIIa regulates the structure of the fibrin clot independently of thrombin generation through direct interaction with fibrin. *Blood* 2011;118:3942-3951.
27. Renne T, Nieswandt B, Gailani D. The intrinsic pathway of coagulation is essential for thrombus stability in mice. *Blood Cells Molecules and Diseases* 2006;36:148-151.
28. Muller F, Mutch NJ, Schenk WA et al. Platelet Polyphosphates Are Proinflammatory and Procoagulant Mediators In Vivo. *Cell* 2009;139:1143-1156.
29. Nielsen VG, Cohen BM, Cohen E. Effects of coagulation factor deficiency on plasma coagulation kinetics determined via thrombelastography (R): critical roles of fibrinogen and factors II, VII, X and XII. *Acta Anaesthesiologica Scandinavica* 2005;49:222-231.
30. Kenne E, Nickel KF, Long AT et al. Factor XII: a novel target for safe prevention of thrombosis and inflammation. *J.Intern.Med.* 2015

31. Schmaier AH. The contact activation and kallikrein/kinin systems: pathophysiologic and physiologic activities. *Journal of Thrombosis and Haemostasis* 2016;14:28-39.

32. Bjorkqvist J, de Maat S, Lewandrowski U et al. Defective glycosylation of coagulation factor XII underlies hereditary angioedema type III. *Journal of Clinical Investigation* 2015;125:3132-3146.

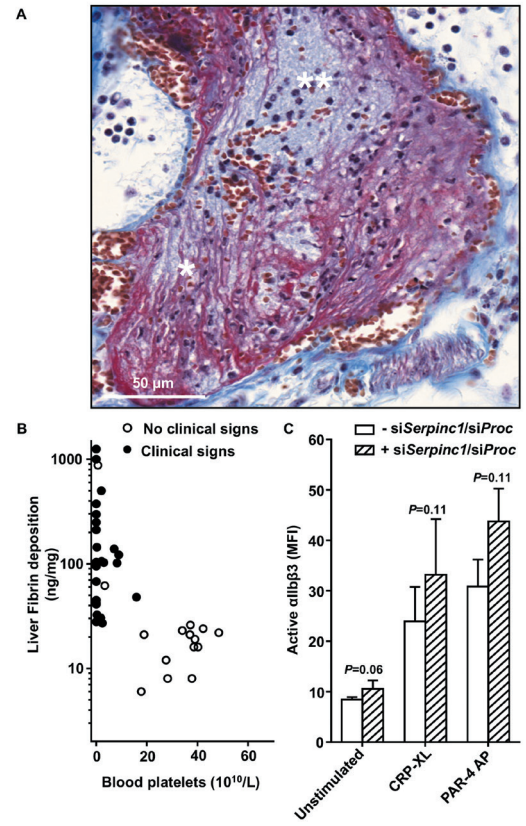

Supplementary figure S1 | Platelets in spontaneous venous thrombosis in mice. A, Venous thrombus in the head (masseter and mandibular area) of a si*Serpinc1*/si*Proc* injected mouse for which paraffin-embedded section was stained according to the Carstairs' method. This methods stains fibrin bright red/pink, platelets navy blue, erythrocytes orange/red, collagen clear blue, and nuclei dark blue/purple. Platelets are abundantly present in the thrombus and localize between the alignment of structures identified as fibrin (single white asterisk) and also co-localize with leukocytes (double white asterisk). White bar indicates 50µm. B, Blood platelets numbers related to liver fibrin deposition for animals treated with si*Serpinc1*/si*Proc* featuring spontaneous venous thrombosis (filled circles) or not (yet) (open circles). Data are pooled from three different experiments (total 38 animals). For reference, normal C57Black/6J female mice (injected solely with siNEG; n=6) have no or low liver fibrin deposition i.e. 4.5 ng/mg (3.1, 5.7) and blood platelet levels numbers of 61x1010/L (54x1010, 64x1010). C, Blood platelet activation before onset of the thrombotic coagulopathy i.e. 48 hours after si*Serpinc1*/si*Proc* treatment (+si*Serpinc1*/si*Proc*, n=5 animals), compared to a non-treated control group of mice (PBS injection, -si*Serpinc1*/si*Proc*, n=4 animals). Flow cytometry analysis was performed to determine the expression (median fluorescence intensity, MFI) of the platelet surface marker active integrin αIIbβII in absence or presence of a (ex vivo) stimulus i.e. cross-linked collagen-related peptide (CRP-XL, 0.25µg/mL) or protease-activated receptor-4 activation peptide (PAR-4 AP, 0.1mM). Expression (MFI) of P-selectin, another platelet surface marker, yielded comparable results (data not shown). *P*-values indicate differences in expression observed for – and +si*Serpinc1*/si*Proc* animals (Mann Whitney Rank-sum test).

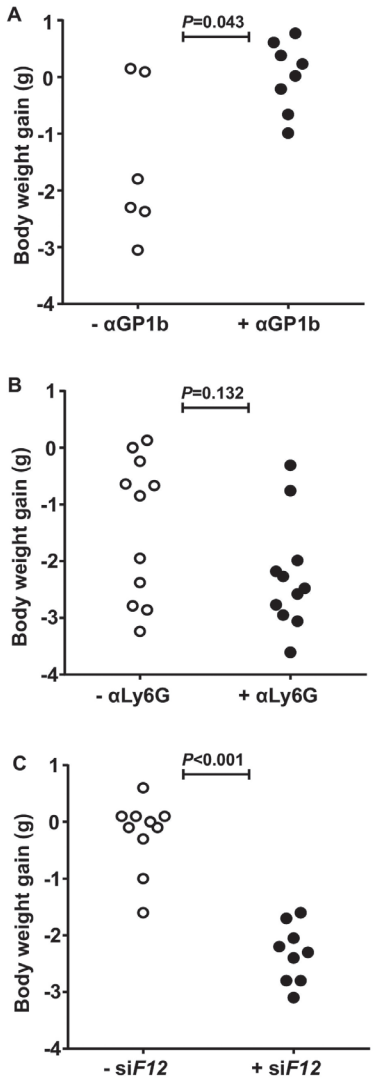

Supplementary figure S2 | Net mice body weight gain after si*Serpinc1* and si*Proc* injection. A, Body weight gain 3 days after si*Serpinc1*/si*Proc* treatment. One of the mice from the -αGP1b-group died because of the thrombotic coagulopathy. -αGP1b (si*Serpinc1*/si*Proc* -αGP1b, open circles): -2.05g (-3.05, 0.11), +αGP1b (si*Serpinc1*/si*Proc* +αGP1b, black circles): 0.13g (-0.99, 0.77). *P*=0.043, Mann Whitney Rank-sum test. B, Body weight gain 3 days after si*Serpinc1*/si*Proc* treatment. One of the mice from both groups (-αLy6G and +αLy6G) died because of the thrombotic coagulopathy. –αLy6G (si*Serpinc1*/si*Proc* -αLy6G, open circles): -0.85g (-3.24, 0.13), +αLy6G (si*Serpinc1*/si*Proc* +αLy6G, black circles): -2.48g (-3.61, -0.31). *P*=0.132, Mann Whitney Rank-sum test. C, Body weight gain 2 days after si*Serpinc1*/si*Proc* treatment. -si*F12* (si*Serpinc1*/si*Proc* -si*F12*, open circles): -0.05g (-1.60, 0.60), +si*F12* (si*Serpinc1*/si*Proc* +si*F12*, black circles): -2.30g (-3.10, -1.60). *P*<0.001, Mann Whitney Rank-sum test. Data are presented as the median with the range (minimum and maximum, respectively).

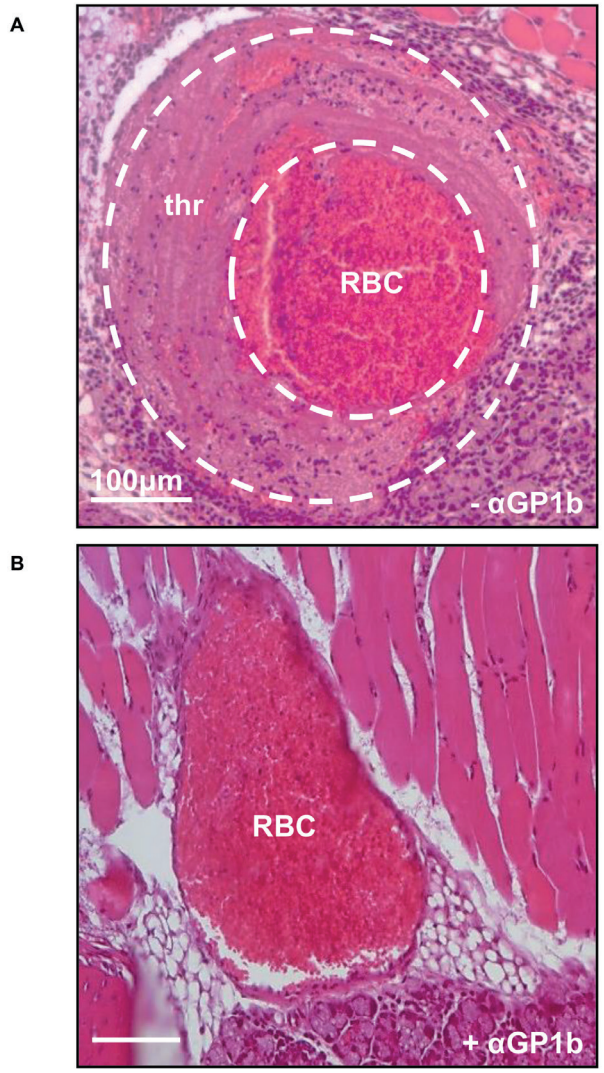

Supplementary figure S3 | Blood vessels in si*Serpinc1*/si*Proc* -αGP1b and si*Serpinc1*/si*Proc* + αGP1b mice. Representative thrombus identified in a vein in the control group (-αGP1b, panel C), and a representative vein in the platelet depleted group (+αGP1b, panel D) in H&E stained sections. In panel A, the white scattered lines marks the area identified as a thrombus. rbc: postmortem clotted blood rich in red blood cells, thr: thrombus. White lines indicates 100 µm. Please note, panels represent the same sections as figures 1C and 1D.

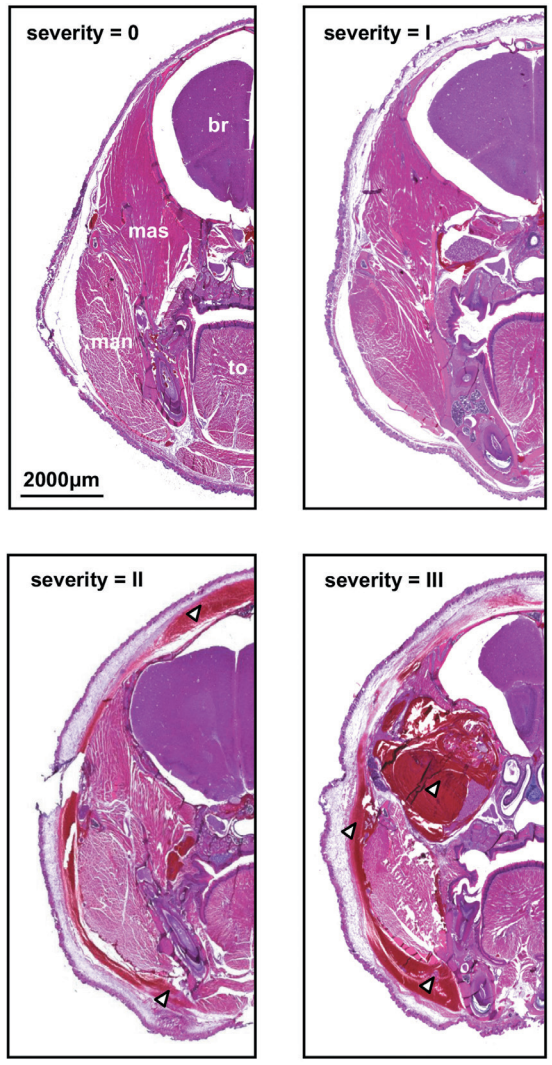

Supplementary figure S4 | Coronal sections of mice heads, representative for four different severity categories. Category 0: Unaffected, category I-III: increasing scores are based on hemorrhages, thrombotic lesions, and edema. For orientation of the selected section (left upper panel), br: Brain, to: Tongue, mas: Masseter muscle, man: Mandibular maxilaris. Black line indicates 2000 µm. Black/white arrowheads indicate bleedings. Please note, lower panels represent the same sections as figures 3C and 3D.

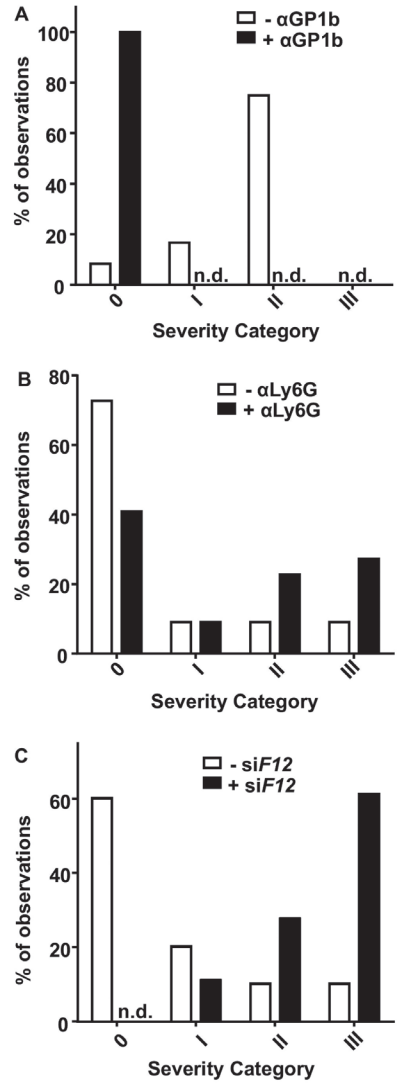

Supplementary figure S5 | Severity scoring for individual mice, divided in four categories, 0-III, see figure S2. A, Severity scores of head sections of mice from the - αGP1b group (si*Serpinc1*/si*Proc* -αGP1b, open circles, n=10) and the +αGP1b group (si*Serpinc1*/si*Proc* +αGP1b, black circles, n=16). n.d. not detected. B, Severity scores of head sections of mice from the –αLy6G group (si*Serpinc1*/si*Proc* -αLy6G, open circles, n=22) and the +αLy6G group (si*Serpinc1*/si*Proc* +αLy6G, black circles, n=20). C, Severity scores of head sections of mice from the –si*F12* group (si*Serpinc1*/si*Proc* -si*F12*, open circles, n=20) and the +si*F12* group (si*Serpinc1*/si*Proc* +si*F12*, black circles, n=18). n.d. not detected. Because of the mostly unilateral nature of lesions, two semi-quantitative scores were granted per mouse during both scoring systems (one left and one right in the head).

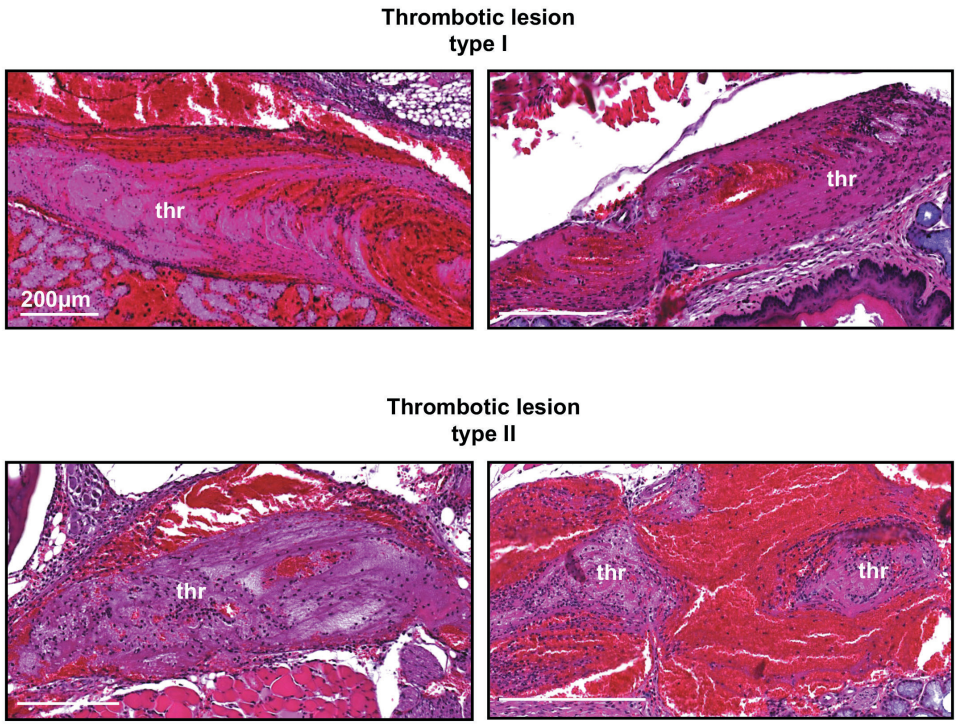

Supplementary figure S6 | Representative sections of mice heads for two different thrombus categories. Thrombi were divided into two different types (blinded analyses, two observers). Thrombus categories were distinguished based on the presence of (I, upper panels) typical organized thrombi within a (mostly) intact venous vessel with layered structures microscopically identified as eosin-positive fibrin, and (II, lower panels) clear structures identified as fibrin (thrombi) embedded or surrounded in red blood cells lacking a typical layered structure. In the latter, no clear vessel structures were identified due to possible vein rupture. The veins around the cranial part of the trachea and the masseter and mandibula maxillaris muscle area were analyzed to score thrombus types, since thrombotic lesions and bleedings were reproducibly found here. thr: Fibrin-rich thrombus. White bars indicate 200 µm.

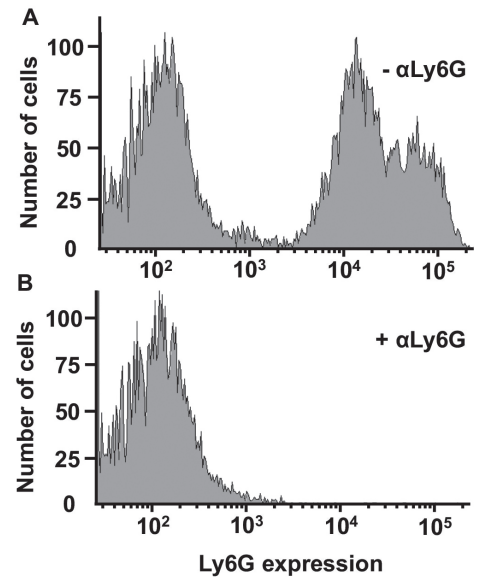

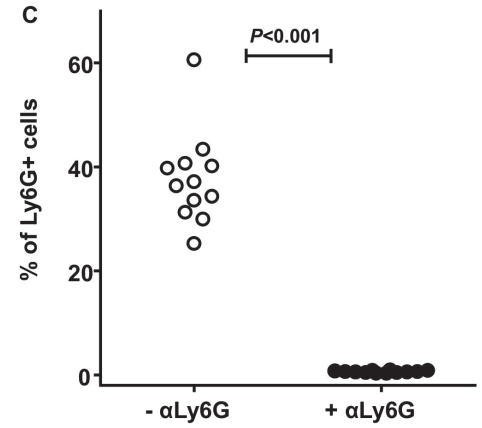

Supplementary figure S7 | Analysis of Ly6G-positive cells in whole blood 1 day after antibody injection using flow cytometry. A/B, Representative analysis of Ly6G expression in viable leukocytes of samples from groups treated with an isotype IgG control antibody (si*Serpinc1*/si*Proc* -αLy6G, panel A) and an Ly6G-depleting antibody (si*Serpinc1*/si*Proc* +αLy6G, panel B). C, Percentage of Ly6G-positive cells from the viable leukocyte population, –αLy6G (si*Serpinc1*/si*Proc* -αLy6G, open circles): 36.80 % Ly6G+ cells (25.30, 60.60), +αLy6G (si*Serpinc1*/si*Proc* +αLy6G, black circles): 0.65% Ly6G+ cells (0.40, 1.00). *P*<0.001, Mann Whitney Rank-sum test. Data are presented as the median with the range (minimum and maximum, respectively).

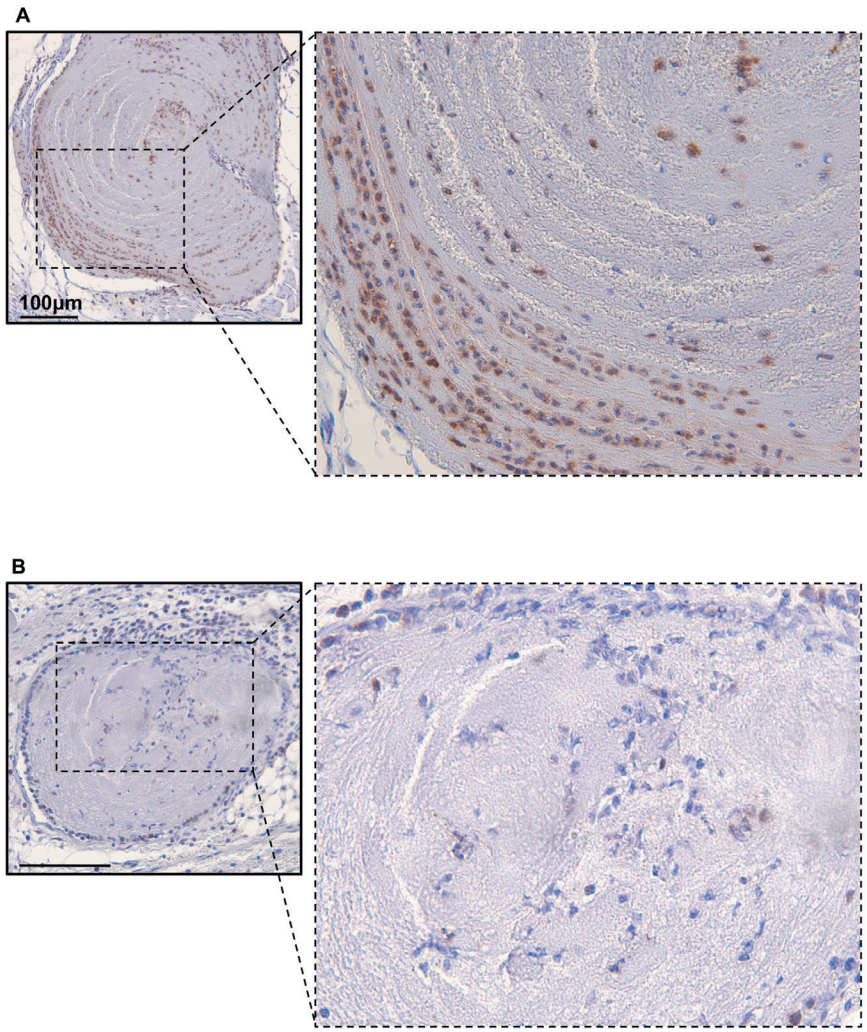

Supplementary figure S8 | Ly6G staining of thrombi found in sections of the head. In the -αLy6G (si*Serpinc1*/si*Proc* -αLy6G, panel A) and +αLy6G (si*Serpinc1*/si*Proc* +αLy6G, panel B) treated mice. Hematoxylin was used for counterstaining, black lines indicate 100 µm. Please note, panels represent the same sections as figures 2C and 2D.

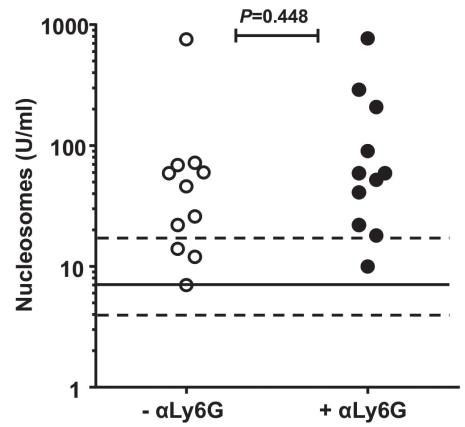

Supplementary figure S9 | Levels of nucleosomes in plasma. Samples were obtained upon sacrifice. – αLy6G (si*Serpinc1*/si*Proc* -αLy6G, open circles): 46 U/ml (7, 756), +αLy6G (si*Serpinc1*/si*Proc* +αLy6G, black circles): 59 U/ml (10, 771), *P*=0.448, Mann Whitney Rank-sum test. Solid and dashed lines indicate nucleosome levels found in uninjected C57BL/6J female mice (median and range, resp. 7 U/ml (4, 17)). Data are presented as the median with the range (minimum and maximum, respectively).